HHS Public Access

Author manuscript

Plast Reconstr Surg. Author manuscript; available in PMC 2023 May 03.

Published in final edited form as:

Plast Reconstr Surg. 2023 January 01; 151(1): 72e–84e. doi:10.1097/PRS.0000000000009798.

Fluidic device system for mechanical processing and filtering of human lipoaspirate *ex vivo* enhances recovery of mesenchymal stem cells in comparison to standard nanofat processing

Jeremy A. Lombardo, PhD[1], **Derek A. Banyard, MD, MBA, MS**[4,5], **Alan D. Widgerow, MBBCh, MMed**[4,5], **Jered B. Haun, PhD**[1,2,3,6,7]

[1]Department of Biomedical Engineering, University of California Irvine, Irvine, CA 92697, USA.

[2]Department of Chemical and Biomolecular Engineering, University of California Irvine, Irvine, CA 92697, USA.

[3]Department of Materials Science and Engineering, University of California Irvine, Irvine, CA 92697, USA.

[4]Department of Plastic Surgery, School of Medicine, University of California, Irvine, Orange, CA 92868, USA

[5]Center for Tissue Engineering, University of California, Irvine, Orange, CA 92868, USA.

[6]Chao Family Comprehensive Cancer Center, University of California Irvine, Orange, CA 92868, USA.

[7]Center for Advanced Design and Manufacturing of Integrated Microfluidics, University of California, Irvine, Irvine, CA, 92697, USA.

Abstract

Background: Adipose tissue is an easily accessible source of stem and progenitor cells that offers exciting promise as an injectable autologous therapeutic for regenerative applications. Mechanical processing is preferred over enzymatic digestion, and the most common method involves shuffling lipoaspirate (LA) between syringes and filtering to produce nanofat (NF). While NF has shown exciting clinical results, we hypothesized that new device designs could enhance recovery of stem/progenitor cells through optimization of fluid dynamics principles, integration, and automation.

Methods: We designed and fabricated the Emulsification and Micronization Device (EMD) and the Filtration Device (FD) to replace the manual NF procedures. Using human LA samples, the EMD and FD were optimized and compared to traditional NF using *ex vivo* measurements of cell

Corresponding author: Jered B. Haun, PhD, Department of Biomedical Engineering, University of California Irvine, 3107 Natural Sciences II, Irvine, CA, 92697, jered.haun@uci.edu, http://haun.eng.uci.edu.

Author Contributions

J.A.L., D.A.B, A.D.W., and J.B.H. devised the concept for the work. J.A.L and J.B.H. designed the fluidic device technologies. J.A.L. carried out the experimental work. All authors carried out the experimental analysis. J.A.L. and J.B.H. wrote the manuscript, which all authors reviewed and edited.

Accepted for presentation at: Plastic Surgery Research Council Annual Meeting (PSRC) 2020, Toronto, Canada; *cancelled due to Covid-19

number, viability, and percentage of mesenchymal stem cells (MSCs) and endothelial progenitor cells (EPCs).

Results: The EMD produced statistically similar results to NF, and these findings were confirmed for a cohort of diabetic patients. Combining the FD with the EMD was superior to manually filtered NF both in terms of recovered cell percentages (>1.5-fold) and numbers (2 to 3-fold). Differences were statistically significant for total MSCs and a DPP4+/CD55+ sub-population linked to improved wound healing in diabetes.

Conclusions: The new EMD and FD devices improved mechanical processing of human LA in terms of MSC enrichment and number compared to traditional NF. Future work will seek to investigate the wound healing response both *in vitro* and *in vivo*, as well as refine the technology for automated operation within clinical settings.

INTRODUCTION

Interest is rapidly growing to utilize adipose tissue as a potent, easily accessible source of regenerative cells for injectable autologous therapies, as evidenced by the increasing number of clinical trials and commercial isolation systems.[1] Adipose-derived stem cells (ADSCs) are a subset of mesenchymal stem cells with adipogenic, osteogenic, and chondrogenic differentiation potential.[2–4] ADSCs have been shown to improve regeneration in bone,[5] cartilage,[6] cardiac tissue,[7] and other organs,[8] as well as treat rheumatoid arthritis and Crohn's disease.[9,10] Adipose tissue is obtained via tumescent liposuction, and this lipoaspirate (LA) is often treated with proteolytic enzymes such as collagenase to release cells that comprise the stromal vascular fraction (SVF). SVF includes mature cells such as fibroblasts, endothelial cells, pericytes, and macrophages, regenerative cells such as MSCs and endothelial progenitor cells (EPCs), and contaminating blood cells. Importantly, SVF has been shown to exhibit comparable regenerative capabilities to ADSCs, including improved healing of burns, scars, and ischemic wounds in diabetes and other chronic diseases.[11–17]

Enzymatic digestion of adipose tissue presents regulatory challenges,[18] and may not produce optimal SVF from a therapeutic standpoint. This has led to the development of mechanical methods to liberate SVF without the use of enzymes. A common method involves repeatedly passing LA back and forth between two syringes resulting in an emulsion termed nanofat (NF).[19] After a filtration step, NF is injected and has been shown to be effective in correcting superficial rhytides, scars and discoloration, as well as improving neovascularization and fat graft survival.[19–21] We recently characterized the cellular composition of NF, and demonstrated that stem and progenitor cell populations were enriched by mechanical processing.[22] Specifically, we observed at least three-fold increases in the percentage of MSCs, EPCs, and a subset of MSCs called multi-lineage differentiating stress-enduring (MUSE) cells, which exhibit pluripotency.[23–25] While these results are exciting, the NF method was originally based on standard laboratory supplies and manual steps, and there has been little change to the format. Commercial systems such as the Tulip and LipoCube[26] still require LA to be manually pushed by hand between two syringes, with a coupler dictating the effectiveness of micronization. This is followed by a second manual filtering step. Thus, it remains to be seen whether new design concepts can improve the

NF process. Moreover, automation could reduce variability introduced by human operators. Other mechanical methods have been developed, including centrifuging, shaking, vortexing, and commercial products such as Lipogems.[27–29] However, these methods require even more manual steps and/or laboratory equipment, which is not conducive to clinical settings.

Microfluidic technologies have made it possible to rapidly design and test new concepts for manipulating fluids on the size scale of tissues and cells.[30,31] In previous work, we developed microfluidic device technologies to dissociate tissues into single cells. This included a digestion device to break down tissue using hydrodynamic fluid shear and proteolytic enzymes,[32] a dissociation device to reduce cellular aggregates into single cells using a network of branching channels with repeated expansions and constrictions,[33,34] and a filter device to eliminate remaining aggregates using nylon mesh membranes.[35] We also discovered that the filter device increased cell recovery by two- to three-fold for digested murine kidney, tumor, and liver via a dissociation mechanism. Recently, we integrated all three tissue processing technologies into a single platform and demonstrated at least two-fold enhancement of cell recovery for different organs and improved reliability over manual methods.[36] We hypothesized that these results would extend to mechanical processing of human LA. Specifically, we hypothesized that the micronization step could be improved by optimally leveraging laminar fluid shear forces to break down tissue and turbulent fluid mixing to emulsify lipid droplets. Additionally, integration and replacement of manual steps would improve reliability and lead to the development of a fully automated benchtop system.

Here, we present a novel fluidic device system for mechanically processing adipose tissue into an injectable therapeutic (Figure 1). We first designed an Emulsification and Micronization Device (EMD) to enhance mechanical processing relative to the inter-syringe method used to produce NF. We also designed a new Filtration Device (FD) to remove the largest adipose tissue fragments from mechanically processed LA and to further maximize recovery of stem and progenitor cells. These devices were combined, operated using a pump rather than manual actuation, and processing performance was compared to enzymatic digestion and NF processing for stem and progenitor cell recovery.

MATERIALS AND METHODS

This study was conducted in accordance with the regulations of the Institutional Review Boards at the University of California, Irvine (no. 2015–2181) and Long Beach VA Hospital (no. 01308). Patients were recruited who were undergoing liposuction for either cosmetic or reconstructive. Active systemic infection or use of immunosuppressive therapy resulted in exclusion from participation. A total of 13 patients were recruited for this study. Four patients had diabetes of unknown type, including 2 female and 2 male, with an average age of 61.5 (range, 59–63). Both female and male diabetic cohorts were split between African American and Caucasian descent. Nine patients were otherwise healthy, including all female, with an average age of 51.4 (range, 39–76). Four were Caucasian (44.4%), two Latina (22.2%), and three of Asian descent (33.3%). Adipose specimens were collected from the abdomen and/or flanks using standard vacuum-assisted liposuction with a 3 or 3.7 mm harvest cannula, and kept at room temperature until use.

Emulsification and Micronization Device (EMD) Design, Fabrication, and Operation

The EMD features two 1.5 mm diameter constrictions that are separated by an abrupt expansion (Figure 2A). The constrictions generate shear forces that break down tissue into smaller units. Based on the high viscosity of LA, we expect laminar flow within the constrictions, which will provide consistent and reliable shear forces for micronization. The rapid expansion is designed to provide turbulent mixing to emulsify the fatty oil layer. Devices were 3D printed by Dinsmore Inc. (Irvine, CA) as a single part using an SLA 3D printer and biocompatible Somos BioClear resin (Royal DSM, Elgin, Illinois). 3D printing was chosen to produce a single monolithic construct that could withstand high flow rates and pressures required for LA processing, during which device clogging is commonly experienced. A fabricated device is shown in Figure 2B.

The EMD was evaluated using human LA samples from otherwise normal (N = 5) and diabetic (N = 4) patients. LA was washed with phosphate-buffered saline (PBS) and sub-divided into separate portions. One portion was left unprocessed and termed macrofat (MF). Another portion was processed into NF by manually passing 30 times between two connected syringes, as previously described.[19] Remaining samples were processed with the EMD for 10, 20, or 30 passes using a syringe pump (Harvard Apparatus, Holliston, MA) at a flowrate of 20 mL/s, approximately the same flow rate used to manually produce NF. We employed a high precision syringe pump to ensure that flow rate was as accurate (within 0.35% of set rate) and reproducible (within 0.05% of actual rate) as possible.

Filtration Device (FD) Design, Fabrication, and Operation

The FD captures large, mm-scale pieces of adipose tissue that remain after processing with the EMD. The multi-layer design includes fluidic channels and an embedded nylon mesh membrane (Figure 2C) that were fabricated by ALine, Inc. (Rancho Dominguez, CA) using a commercial laminate approach, similar to previous work.[35] Membrane pore size was either 0.5 or 1 mm, similar that used to filter NF prior to injection.[19] A fabricated device is shown in Figure 2D.

Prior to FD filtration, LA from patients (N = 4) was processed using the EMD using 30 passes. Sample was then passed through using a syringe pump at 10 mL/min. FDs containing either 0.5 or 1 mm nylon mesh membranes were evaluated, and compared to NF that was passed through a 1 mm mesh cloth. Filtered samples were collected from the effluent outlet.

Cell Isolation

Following mechanical processing, cells were isolated from all samples as previously described.[22] Briefly, 0.1% type I collagenase (Sigma-Aldrich Co., St. Louis, MO) was prepared in PBS, sterilized using a 0.22 μm vacuum filter (Millipore Corp., Billerica, MA), mixed with LA at a 1:1 volume ratio, and incubated at 37°C for 30 min in a water bath while swirling intermittently. Control media (DMEM supplemented with 10% fetal bovine serum, 500 IU penicillin, and 500 μg streptomycin) was then added in an equal volume to neutralize enzymatic activity. The mixture was allowed to separate by gravity for 10 minutes, and the infranatant layer that contains SVF was collected and filtered through a 100 μm cell

strainer. Samples were centrifuged at 500 × g for 7 min and pellets were resuspended in control media. Nucleated cell counts and viability were determined using an automated, dual-fluorescence cell counter (Logos Biosystems Inc., Annandale, VA).

Flow Cytometry

Collagenase-digested cell suspensions were evenly divided into FACS tubes and resuspended in FACS Buffer (1× PBS, without Ca and Mg) supplemented with 1% BSA (PBS+). Cell suspensions were stained simultaneously in 100 μL total volume with 5 μL (1 test) of each monoclonal mouse anti-human antibodies shown in Table 1 (all from BioLegend, San Diego, CA). After 20 minutes at 4°C, samples were washed with FACS Buffer by centrifugation, resuspended in PBS+ supplemented with 7-AAD (BD Biosciences, San Jose, CA) for dead cell exclusion, and maintained on ice for at least 15 minutes prior to analysis on a Novocyte 3000 Flow Cytometer (ACEA Biosciences, San Diego, CA). Compensation was determined using single antibody-stained samples and compensation beads (Invitrogen, Waltham, MA). Heat treatment (55°C for 15 min) was used as a dead cell control for 7-AAD. Gates were inputted into FlowJo software (Ashland, OR) to automatically calculate the compensation matrix. Signal positivity was determined using appropriate Fluorescence Minus One (FMO) controls. A sequential gating scheme (Figure, Supplemental Digital Content 1) was used to identify cell populations of interest from non-cellular debris and cellular aggregates. The cell populations of interest are listed and described in Table 2.

Statistics

Data are represented as the mean ± standard error from at least three independent patient samples. Statistical analysis included ANOVA using parametric F tests to evaluate differences among groups and post-hoc parametric t tests to evaluate pairwise differences between groups. We also performed non-parametric Kruskal-Wallis tests to confirm results remained consistent. Differences were considered to be statistically significant when both parametric and non-parametric tests yielded p-values <5%.

RESULTS

The EMD enriches for MSCs and EPCs in a similar manner to NF

We first performed an optimization study for the EMD using human LA samples (N = 5 patients) and different numbers of passages through the device at 20 mL/s via a syringe pump which demonstrated that 30 produced the best results (Figure, Supplemental Digital Content 2). Results for this optimal condition are shown in Figure 3, relative to MF and NF. For total cell recovery, MF samples yielded the highest value at ~730,000 +/− 180,000 cells/mL of LA (Figure 3A). NF and EMD produced lower cell counts, by nearly half, but differences were not statistically significant. Viability was similar, at ~90%, for all conditions (Figure 3B), with no statistically significant differences. The relative percentage of stem/progenitor populations recovered in cell suspensions are shown in Figure 3C. Results were normalized to MF since absolute numbers within SVF have been shown to vary widely across different patients and anatomical locations used to harvest adipose tissue.[37,38] Total MSCs, Muse and DPP4+/CD55+ MSC subpopulations, and EPCs were all enriched in

NF, by 2- to 3-fold, as shown previously.[22] For the EMD, stem/progenitor percentages were generally comparable to NF, and differences were not statistically significance. Statistical comparisons for all outcomes and testing conditions are included in Table, Supplemental Digital Content 1. Population percentage results without normalization to MF were similar (Figure, Supplemental Digital Content 3).

EMD enrichment results extend to diabetic patients

We also evaluated a cohort of diabetic patients (N = 4), and again found that 30 passes through the EMD was optimal (Figure, Supplemental Digital Content 4). Total cell recovery was similar to normal patients (680,000 +/− 240,000), with NF and EMD at approximately half of MF (Figure 4A). These differences were statistically significant based on the parametric F test (p-value=0.038), but not the non-parametric KW test. Viability was similar for all conditions (Figure 4B), with no statistically significant differences. Stem/progenitor cell percentage (Figure 4C) results followed the initial non-diabetic patient cohort, with all MSC and EPC subtypes enriched by >2-fold for both NF and EMD. Statistical comparisons for all outcomes and testing conditions are included in Table, Supplemental Digital Content 2. Non-normalized population percentages were also similar to the initial non-diabetic patient cohort (Figure, Supplemental Digital Content 5).

The FD further enhances enrichment and recovery of MSCs populations

Finally, we performed an optimization study for the FD using human LA samples (N = 4 patients) and filters with different pore sizes, which indicated that 1 mm pores produced more cells and higher percentages of stem/progenitor cells relative to 0.5 mm (Figure, Supplemental Digital Content 6). Cell recovery for the FD with 1 mm pores was lower than using the EMD alone, but we found that manually filtering NF decreased cell recovery and stem/progenitor cell percentages to an even greater extent (Figure, Supplemental Digital Content 6). Filtered results for NF and EMD/FD are shown in Figure 5, relative to MF. A total of 900,000 +/− 160,000 cells were recovered per mL LA from MF after enzymatic digestion (Figure 5A), similar to initial studies. Cell count drastically decreased for manually filtered NF to 130,000 +/− 50,000 cells/mL, while the EMD/FD produced 270,000 +/− 30,000 cells/mL. Differences were statistically significant relative to MF (F test p-value=0.001, KW test p-value=0.013). Cell viability remained high, in excess of 90%, for all conditions (Figure 5B), with no statistically significant differences. Flow cytometry indicated that much of the stem/progenitor cell enrichment attained by NF was lost after filtering (Figure 4C), with population percentages reduced to near MF levels. Conversely, the FD better retained stem/progenitor cell enrichment from EMD conditions, with total CD34+ cells, MSCs, and EPCs all exceeding MF by >2-fold. Importantly, differences between EMD/FD and filtered NF were statistically significant for total MSCs (1.9 +/− 0.2 vs 1.3 +/− 0.04, F test p-value=0.037, KW test p-value=0.021) and the DPP4+/CD55+ MSC subpopulation (1.5 +/− 0.2 vs 0.8 +/− 0.2, F test p-value=0.039, KW test p-value=0.021). We also note that additional EMD/FD-processed populations attained statistical significance for one of the tests, but not both, including CD34+ (2.7 +/− 0.7 vs 1.2 +/− 0.2, F test p-value=0.075, KW test p-value=0.021) and EPCs (5.5 +/− 1.5 vs 2.2 +/− 0.1, F test p-value=0.076, KW test p-value=0.021). Non-normalized population percentages are shown

in Figure, Supplemental Digital Content 7. We note that differences between the EMD/FD and MF did reach statistical significance for EPCs following filtration.

We note that the lower cell recovery obtained after filtering NF in Figure 5A exacerbates the lower relative number of stem/progenitor cells in Figure 4C. To illustrate this point, Figure 4D displays total cell recovery for each stem/progenitor cell type. Results were again normalized to MF, which now represents the expected maximum recovery level. Filtered NF ranged from 10 to 30% of this recovery potential, while EMD/FD was consistently >50%. EPCs exceeded 100%, but the error was large. Critically, differences between NF and EMD/FD reached high level of statistical significance for MSCs (0.6 +/− 0.1 vs 0.2 +/− 0.07, F test p-value=0.020, KW test p-value=0.021) and the DPP4+/CD55+ MSC subpopulation (0.49 +/− 0.9 vs 0.12 +/− 0.06, F test p-value=0.0.104, KW test p-value=0.021). The other populations attained statistical significance for only one test, including CD34+ (0.9 +/− 0.3 vs 0.2 +/− 0.1, F test p-value=0.0.055, KW test p-value=0.021), EPCs (1.8 +/− 0.7 vs 0.3 +/− 0.1, F test p-value=0.068, KW test p-value=0.021), and Muse (0.5 +/− 0.1 vs 0.2 +/− 0.1, F test p-value=0.049, KW test p-value=0.083). Statistical comparisons for all outcomes and testing conditions are provided in Table 3.

DISCUSSION

Human LA contains a mixture of nonuniform-sized tissue fragments, cells, and fatty oils that requires both micronization and emulsification. While the NF method has been shown to be effective at processing LA into an injectable cellular therapeutic without enzymatic treatment, it requires sample to be shuffled between two syringes by hand.[19] The EMD was designed to process LA in a manner similar to NF, but with greater control over flow due to the use of a pump. The design included two constriction regions that were separated by an abrupt expansion, which creates regions of high viscous shear force and turbulent mixing. The EMD resulted in lower total cell recovery relative to MF, which was likely caused by destruction of fragile cells by shear forces, as previously observed during NF processing.[19] However, stem and progenitor cells appear relatively resistant to these shear forces, leading to enrichment in the cell suspensions.[22] In this study, we found that EMD treatment did result in enrichment of MSCs and EPCs relative to MF, statistically similar to NF. These results were replicated using LA from patients with diabetes. Enrichment of stem/progenitor populations is particularly encouraging in the context of diabetes, as wound healing and neovascularization are well known to be impaired.[39] Specifically, diabetes has been shown to deplete key stem cell subpopulations in adipose tissue,[40] which highlights the potential impact of enhanced enrichment and recovery.[41]

The FD was designed to work in concert with the EMD, removing any remaining large, mm-scale pieces of adipose tissue that would not be able to pass through small-bore needles. The FD better preserved both total cell recovery and stem/progenitor enrichment in comparison to NF with manual filtration. Specifically, the FD containing a 1 mm membrane produced >2-fold more total cells and greater enrichment levels for all stem/progenitor cells studied. Most importantly, these two effects combined to increase the total number of stem/progenitor cells recovered, and this difference was statistically significant for total MSCs and the DPP4+/CD55+ subpopulation, while Muse and EPCs were at the borderline

of significance. This implies that most NF-processed cells are lost during the filtration step, and thus excluded from the final injectable therapeutic. Conversely, 2- to 3-fold more stem/progenitors will be present in cell suspensions generated with the EMD/FD. Interestingly, we found that EPCs were higher after EMD/FD treatment in comparison to MF, which should not be possible since MF was not filtered. This difference was not significant, but could suggest that our fluidic device system is more effective at dissociating tissues than enzymatic treatment alone, as we have observed in our previous work.[32,42–44] We will follow up on this finding in future studies.

We acknowledge that the strongest effect that we observed in this study was for the FD following EMD treatment. We suspect that enhanced processing by the EMD played a role, but at this time we do not know whether the FD would similarly improve cell recovery for NF. It is also unclear how the FD would compare to commercial filtration systems such as the Tulip and Lipocube following either EMD or NF.[26] These questions will all be studied in future work. We do note that our results were obtained using a syringe pump, obviating the need for manual contribution from a human operator, which can introduce variability, and in general presents a challenge to generating consistent and reproducible flow rates and shear forces. This could, in turn, negatively affect the quality of the final cell suspension. Migrating to a pump-driven system will help to standardize and automate the processing of LA for clinical settings. Our EMD and FD technologies were designed to function as disposable cartridges for such an automated system, which will be developed and tested in future work.

Limitations to this study include patient-to-patient variability with respect to the number of cells recovered from LA for various cell subpopulations. While MF normalization did provide clear evidence of the effects of mechanical processing and filtration, we will seek to confirm these findings in larger cohorts, including patients with both type 1 and type 2 diabetes. Notably, we have only assessed stem/progenitor cell enrichment and recovery number, and thus future work will seek to directly assess pro-healing responses *in vitro*, using animal models, and, after obtaining regulatory approval, in human subjects. Finally, we have focused on injectable cellular therapeutics, but NF has also been explored for fat grafting, and it has been shown that downstream processing such as staged centrifugation can concentrate MSCs.[45] Alternative processing methods and applications, such as fat grafting, will be investigated in future studies.

CONCLUSION

In this work, we have presented and characterized a set of new fluidic devices that mechanically processes human LA via emulsification, micronization, and filtering into a format that can be injected directly as a cell-based therapeutic. This system is similar to NF, but significantly enhances MSCs and EPCs in terms of cell numbers and relative concentration. Fluid is also driven using a pump instead of manual actuation, which holds the potential for automating and standardizing LA processing in the clinical setting. Future work will seek to evaluate whether the findings here translate to improved wound healing using *in vitro* and *in vivo* models, as well as to develop out an automated benchtop system.

Supplementary Material

Refer to Web version on PubMed Central for supplementary material.

Acknowledgements

The authors would like to thank Dr. Keyianoosh Paydar, Dr. Garrett Wirth, and the Department of Plastic Surgery at the University of California, Irvine for support and assistance with specimen collection. We also thank Dr. Tuyen Hoang of the Biostatistics, Epidemiology, and Research Design Unit of the Institute for Clinical and Translational Sciences for performing statistical analyses.

Financial Disclosure Statement:

Dr. Banyard is co-founder and former Chief Medical Officer at Syntr Health Technologies, Inc. He is also a paid consultant for Recros Medica, Inc. Dr. Widgerow is Chief Medical Officer of Alastin Inc, as well as a royalty recipient of Allergan CA and LITHA Healthcare South Africa, but has no conflicting interests with this study. Dr. Haun is Chief Science Officer of Kino Discovery, but has no conflicting interests with this study. Dr. Lombardo has nothing to disclose. Funding support was received from the National Center for Research Resources and the National Center for Advancing Translational Sciences, National Institutes of Health, through Grant UL1 TR001414, and the Plastic Surgery Foundation® through the National Endowment for Plastic Surgery Grant PSF-207585. The content is solely the responsibility of the authors and does not necessarily represent the official views of the NIH or the PSF.

REFERENCES

1. Chu DT, Nguyen Thi Phuong T, Tien NLB, et al. Adipose Tissue Stem Cells for Therapy: An Update on the Progress of Isolation, Culture, Storage, and Clinical Application. J Clin Med 2019;8. [PubMed: 31861531]
2. Zuk PA, Zhu M, Mizuno H, et al. Multilineage cells from human adipose tissue: implications for cell-based therapies. Tissue Eng 2001;7:211–228. [PubMed: 11304456]
3. Bunnell BA, Flaat M, Gagliardi C, Patel B, Ripoll C Adipose-derived stem cells: isolation, expansion and differentiation. Methods 2008;45:115–120. [PubMed: 18593609]
4. Gimble JM, Katz AJ, Bunnell BA Adipose-derived stem cells for regenerative medicine. Circ Res 2007;100:1249–1260. [PubMed: 17495232]
5. Godoy Zanicotti D, Coates DE, Duncan WJ In vivo bone regeneration on titanium devices using serum-free grown adipose-derived stem cells, in a sheep femur model. Clin Oral Implants Res 2017;28:64–75. [PubMed: 26853552]
6. Latief N, Raza FA, Bhatti FU, Tarar MN, Khan SN, Riazuddin S Adipose stem cells differentiated chondrocytes regenerate damaged cartilage in rat model of osteoarthritis. Cell Biol Int 2016;40:579–588. [PubMed: 26888708]
7. Valina C, Pinkernell K, Song YH, et al. Intracoronary administration of autologous adipose tissue-derived stem cells improves left ventricular function, perfusion, and remodelling after acute myocardial infarction. Eur Heart J 2007;28:2667–2677. [PubMed: 17933755]
8. Frese L, Dijkman PE, Hoerstrup SP Adipose Tissue-Derived Stem Cells in Regenerative Medicine. Transfus Med Hemother 2016;43:268–274. [PubMed: 27721702]
9. De Francesco F, Romano M, Zarantonello L, et al. The role of adipose stem cells in inflammatory bowel disease: From biology to novel therapeutic strategies. Cancer Biol Ther 2016;17:889–898. [PubMed: 27414952]
10. Garimella MG, Kour S, Piprode V, et al. Adipose-Derived Mesenchymal Stem Cells Prevent Systemic Bone Loss in Collagen-Induced Arthritis. J Immunol 2015;195:5136–5148. [PubMed: 26538398]
11. Nguyen A, Guo J, Banyard DA, et al. Stromal vascular fraction: A regenerative reality? Part 1: Current concepts and review of the literature. J Plast Reconstr Aesthet Surg 2016;69:170–179. [PubMed: 26565755]

12. Guo J, Nguyen A, Banyard DA, et al. Stromal vascular fraction: A regenerative reality? Part 2: Mechanisms of regenerative action. J Plast Reconstr Aesthet Surg 2016;69:180–188. [PubMed: 26546112]
13. Cianfarani F, Toietta G, Di Rocco G, Cesareo E, Zambruno G, Odorisio T Diabetes impairs adipose tissue-derived stem cell function and efficiency in promoting wound healing. Wound repair and regeneration : official publication of the Wound Healing Society [and] the European Tissue Repair Society 2013;21:545–553.
14. Han S, Sun HM, Hwang KC, Kim SW Adipose-Derived Stromal Vascular Fraction Cells: Update on Clinical Utility and Efficacy. Crit Rev Eukaryot Gene Expr 2015;25:145–152. [PubMed: 26080608]
15. Semon JA, Zhang X, Pandey AC, et al. Administration of murine stromal vascular fraction ameliorates chronic experimental autoimmune encephalomyelitis. Stem cells translational medicine 2013;2:789–796. [PubMed: 23981726]
16. Lee HC, An SG, Lee HW, et al. Safety and effect of adipose tissue-derived stem cell implantation in patients with critical limb ischemia: a pilot study. Circ J 2012;76:1750–1760. [PubMed: 22498564]
17. Atalay S, Coruh A, Deniz K Stromal vascular fraction improves deep partial thickness burn wound healing. Burns 2014;40:1375–1383. [PubMed: 24572074]
18. Banyard DA, Salibian AA, Widgerow AD, Evans GR Implications for human adipose-derived stem cells in plastic surgery. J Cell Mol Med 2015;19:21–30. [PubMed: 25425096]
19. Tonnard P, Verpaele A, Peeters G, Hamdi M, Cornelissen M, Declercq H Nanofat grafting: basic research and clinical applications. Plastic and reconstructive surgery 2013;132:1017–1026. [PubMed: 23783059]
20. Uyulmaz S, Sanchez Macedo N, Rezaeian F, Giovanoli P, Lindenblatt N Nanofat Grafting for Scar Treatment and Skin Quality Improvement. Aesthetic Surgery Journal 2018;38:421–428. [PubMed: 29365061]
21. Yu Q, Cai Y, Huang H, et al. Co-Transplantation of Nanofat Enhances Neovascularization and Fat Graft Survival in Nude Mice. Aesthetic Surgery Journal 2017;38:667–675.
22. Banyard DA, Sarantopoulos CN, Borovikova AA, et al. Phenotypic Analysis of Stromal Vascular Fraction after Mechanical Shear Reveals Stress-Induced Progenitor Populations. Plastic and reconstructive surgery 2016;138:237e–247e.
23. Heneidi S, Simerman AA, Keller E, et al. Awakened by cellular stress: isolation and characterization of a novel population of pluripotent stem cells derived from human adipose tissue. PLoS One 2013;8:e64752. [PubMed: 23755141]
24. Kinoshita K, Kuno S, Ishimine H, et al. Therapeutic Potential of Adipose-Derived SSEA-3-Positive Muse Cells for Treating Diabetic Skin Ulcers. Stem cells translational medicine 2015;4:146–155. [PubMed: 25561682]
25. Ogura F, Wakao S, Kuroda Y, et al. Human adipose tissue possesses a unique population of pluripotent stem cells with nontumorigenic and low telomerase activities: potential implications in regenerative medicine. Stem Cells Dev 2014;23:717–728. [PubMed: 24256547]
26. Tiryaki KT, Cohen S, Kocak P, Canikyan Turkay S, Hewett S In-Vitro Comparative Examination of the Effect of Stromal Vascular Fraction Isolated by Mechanical and Enzymatic Methods on Wound Healing. Aesthet Surg J 2020;40:1232–1240. [PubMed: 32514571]
27. Aronowitz JA, Lockhart RA, Hakakian CS Mechanical versus enzymatic isolation of stromal vascular fraction cells from adipose tissue. Springerplus 2015;4:713. [PubMed: 26636001]
28. Ghiasloo M, Lobato RC, Diaz JM, Singh K, Verpaele A, Tonnard P Expanding Clinical Indications of Mechanically Isolated Stromal Vascular Fraction: A Systematic Review. Aesthet Surg J 2020;40:NP546–NP560. [PubMed: 32358957]
29. Tremolada C, Colombo V, Ventura C Adipose Tissue and Mesenchymal Stem Cells: State of the Art and Lipogems(R) Technology Development. Curr Stem Cell Rep 2016;2:304–312. [PubMed: 27547712]
30. Duncombe TA, Tentori AM, Herr AE Microfluidics: reframing biological enquiry. Nat Rev Mol Cell Biol 2015;16:554–567. [PubMed: 26296163]
31. El-Ali J, Sorger PK, Jensen KF Cells on chips. Nature 2006;442:403–411. [PubMed: 16871208]

32. Qiu X, Westerhof TM, Karunaratne AA, et al. Microfluidic device for rapid digestion of tissues into cellular suspensions. Lab Chip 2017;17:3300–3309. [PubMed: 28850139]
33. Qiu X, De Jesus J, Pennell M, Troiani M, Haun JB Microfluidic device for mechanical dissociation of cancer cell aggregates into single cells. Lab on a chip 2015;15:339–350. [PubMed: 25377468]
34. Qiu X, Huang J-H, Westerhof TM, et al. Microfluidic channel optimization to improve hydrodynamic dissociation of cell aggregates and tissue. Scientific reports, Vol. 8, 2018:2774. [PubMed: 29426941]
35. Qiu X, Lombardo JA, Westerhof TM, et al. Microfluidic filter device with nylon mesh membranes efficiently dissociates cell aggregates and digested tissue into single cells. Lab on a chip 2018;18:2776–2786. [PubMed: 30090895]
36. Lombardo JA, Aliaghaei M, Nguyen QH, Kessenbrock K, Haun JB Microfluidic platform accelerates tissue processing into single cells for molecular analysis and primary culture models. Nat Commun 2021;12:2858. [PubMed: 34001902]
37. Jurgens WJ, Oedayrajsingh-Varma MJ, Helder MN, et al. Effect of tissue-harvesting site on yield of stem cells derived from adipose tissue: implications for cell-based therapies. Cell Tissue Res 2008;332:415–426. [PubMed: 18379826]
38. Philips BJ, Grahovac TL, Valentin JE, et al. Prevalence of endogenous CD34+ adipose stem cells predicts human fat graft retention in a xenograft model. Plastic and reconstructive surgery 2013;132:845–858. [PubMed: 23783061]
39. Brem H, Tomic-Canic M Cellular and molecular basis of wound healing in diabetes. J Clin Invest 2007;117:1219–1222. [PubMed: 17476353]
40. Rennert RC, Sorkin M, Januszyk M, et al. Diabetes impairs the angiogenic potential of adipose derived stem cells by selectively depleting cellular subpopulations. Stem Cell Res Ther 2014;5:79. [PubMed: 24943716]
41. Thomas S, AD W, J, L., et al. Adipose Derived Stem Cells andWound Healing in Patients with Diabetes: a Promising Therapeutic Modality. CellR4 2014;2:e1309.
42. Qiu X, De Jesus J, Pennell M, Troiani M, Haun JB Microfluidic device for mechanical dissociation of cancer cell aggregates into single cells. Lab Chip 2015;15:339–350. [PubMed: 25377468]
43. Qiu X, Huang JH, Westerhof TM, et al. Microfluidic channel optimization to improve hydrodynamic dissociation of cell aggregates and tissue. Sci Rep 2018;8:2774. [PubMed: 29426941]
44. Qiu X, Lombardo JA, Westerhof TM, et al. Microfluidic filter device with nylon mesh membranes efficiently dissociates cell aggregates and digested tissue into single cells. Lab Chip 2018;18:2776–2786. [PubMed: 30090895]
45. Pallua N, Grasys J, Kim BS Enhancement of Progenitor Cells by Two-Step Centrifugation of Emulsified Lipoaspirates. Plastic and reconstructive surgery 2018;142:99–109. [PubMed: 29649059]
46. Sidney LE, Branch MJ, Dunphy SE, Dua HS, Hopkinson A Concise review: evidence for CD34 as a common marker for diverse progenitors. Stem Cells 2014;32:1380–1389. [PubMed: 24497003]
47. Murphy MB, Moncivais K, Caplan AI Mesenchymal stem cells: environmentally responsive therapeutics for regenerative medicine. Exp Mol Med 2013;45:e54. [PubMed: 24232253]
48. Chong MS, Ng WK, Chan JK Concise Review: Endothelial Progenitor Cells in Regenerative Medicine: Applications and Challenges. Stem cells translational medicine 2016;5:530–538. [PubMed: 26956207]
49. Rennert RC, Januszyk M, Sorkin M, et al. Microfluidic single-cell transcriptional analysis rationally identifies novel surface marker profiles to enhance cell-based therapies. Nat Commun 2016;7:11945. [PubMed: 27324848]

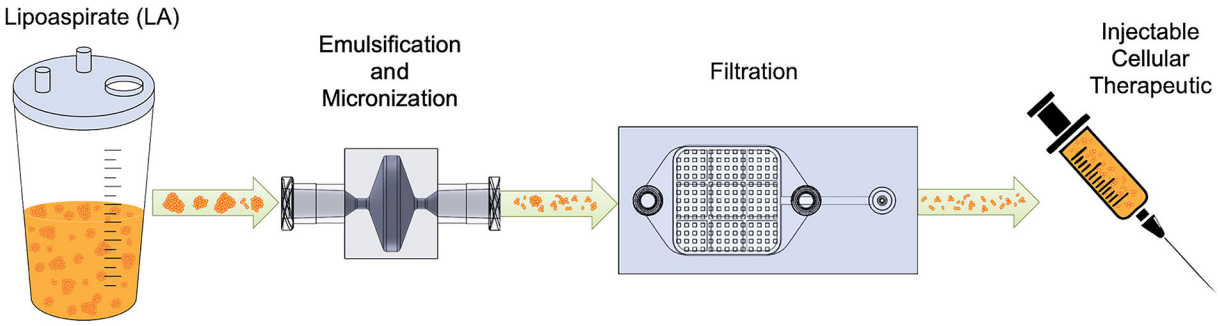

Figure 1. Fluidic devices for processing adipose tissue.

Lipoaspirate (LA) is collected by standard vacuum-assisted liposuction and processed using the Emulsification and Micronization Device (EMD), which breaks down adipose tissue into smaller fragments and emulsifies fat droplets. The mechanically sheared and emulsified sample is then passed through the Filtration Device (FD) to remove the largest tissue pieces, which can clog needles during injection. Following device processing, the final cellular suspension can be injected into a patient for augmenting wound healing or other regenerative capacity.

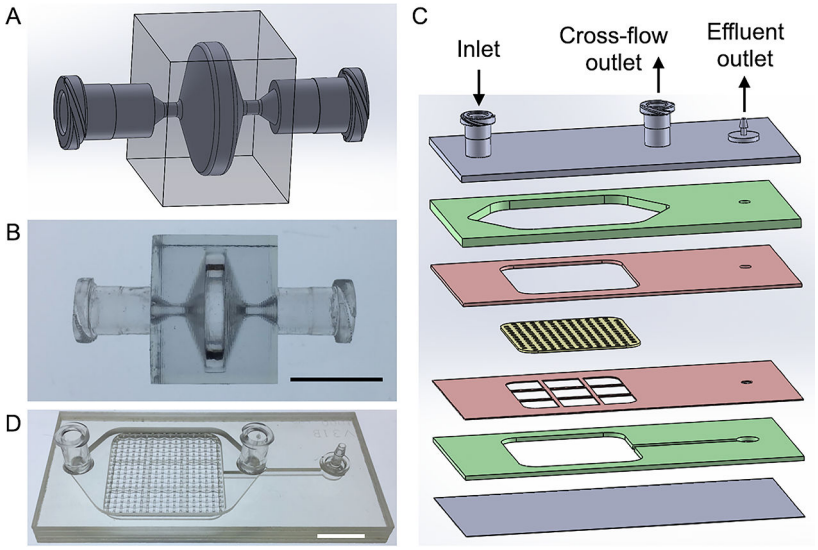

Figure 2. Processing device design and fabrication.

(A,B) Emulsification and Micronization Device (EMD) for processing LA. (A) Schematic of design and (B) picture of device produced via 3D printing. (C,D) Filtration Device (FD) for removing large tissue fragments after EMD treatment. (C) Exploded view showing six plastic layers, including two for channels (green), two acting as the filter spacer and support grid (red), and two for sealing the top and bottom of the device. The embedded nylon filter is shown in yellow. (D) Picture of the FD with 1 mm pore nylon filters that was fabricated using pressure lamination. Scale bars are 1 cm.

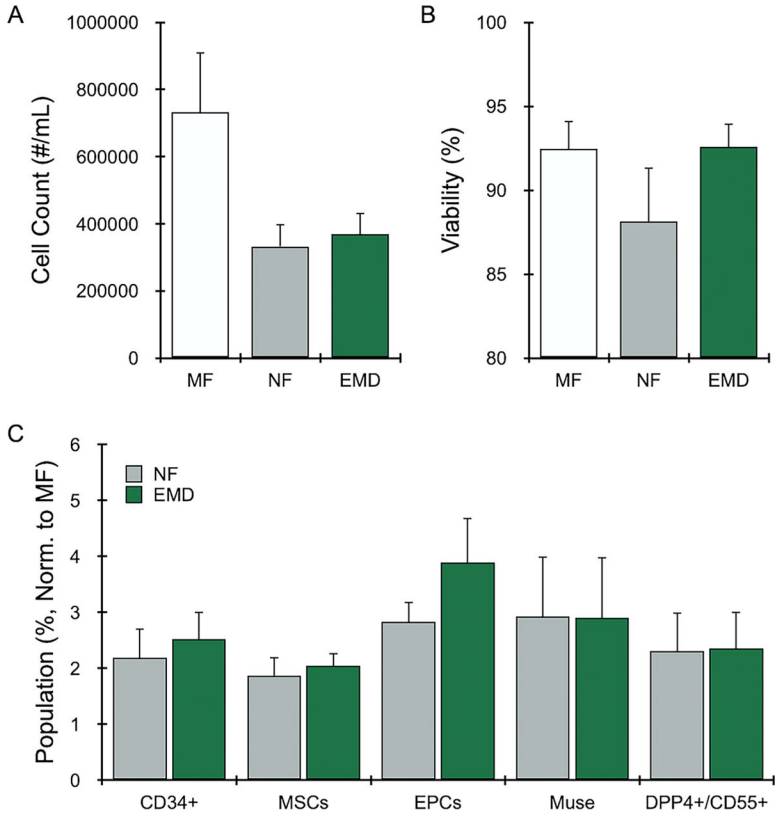

Figure 3. Emulsification and Micronization Device (EMD) results for human LA.

Human LA (N = 5) was mechanically processed by manually shuffling between two syringes (nanofat, NF) or using the EMD with 30 device passes. Unprocessed LA is indicated as macrofat (MF). All samples were digested with collagenase prior to cell analysis. (A) Nucleated cell counts decreased by ~half for NF and all device-processed conditions. (B) Nucleated cell viability remained at ~90% for all conditions. (C) Stem and progenitor cells were identified by flow cytometry, and the relative population percentage was calculated and normalized to MF (value=1). Mechanical processing enriched stem/progenitor cell types of interest, often by 2- to 3-fold compared to MF, while the EMD provided similar or improved results. Error bars represent standard error from at least three independent experiments.

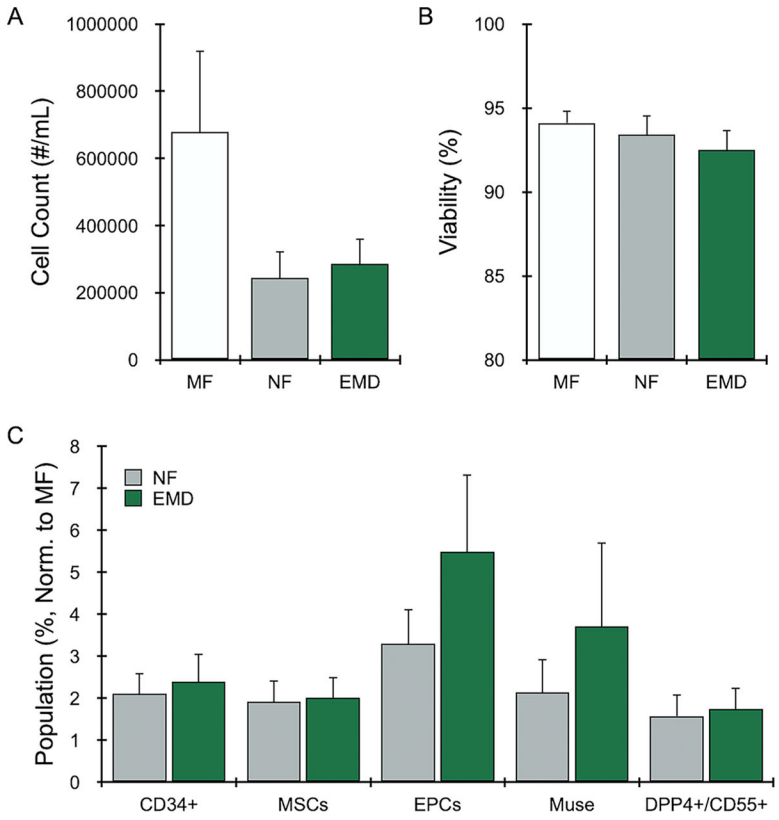

Figure 4. EMD results for diabetic human LA.

Diabetic human LA (N = 4) was mechanically processed as NF or the EMD, or left unprocessed as MF. All samples were digested with collagenase prior to cell analysis. Results for (A) nucleated cell counts, (B) viability, and (C) normalized cell populations closely followed results in Figure 3 for non-diabetic LA samples. Error bars represent standard error from at least three independent experiments.

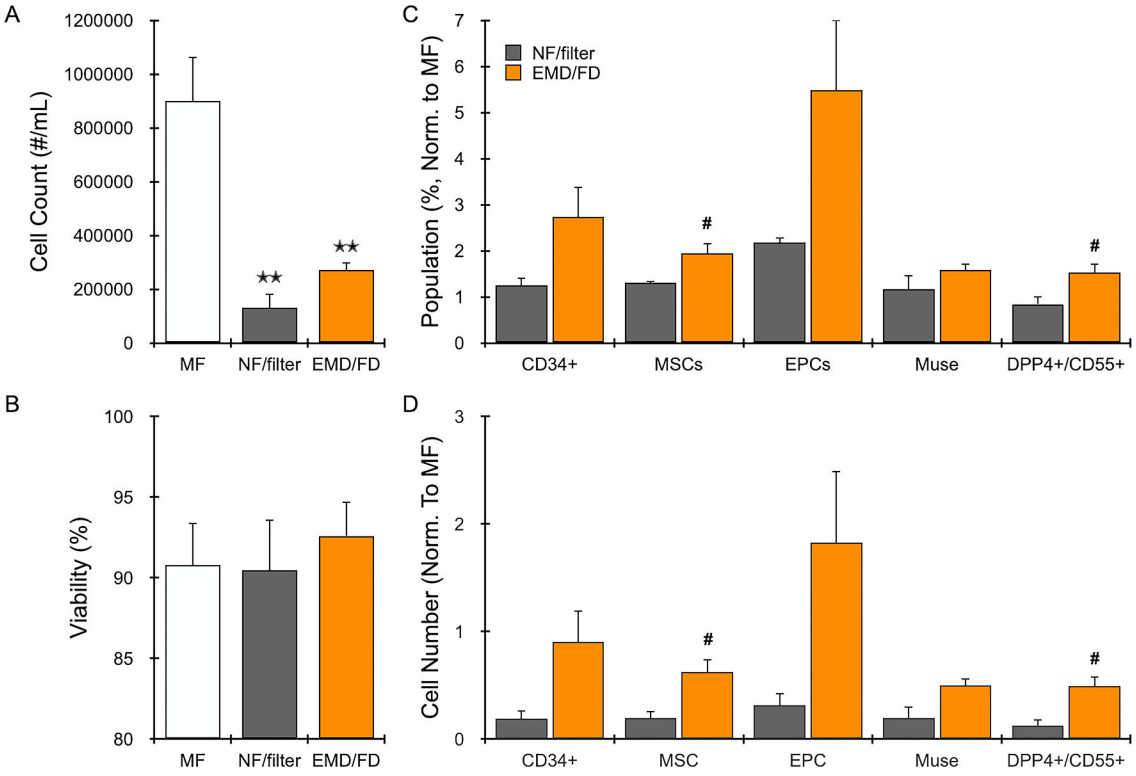

Figure 5. Filtration Device (FD) results.

Human LA (N = 4) was mechanically processed as NF or using the EMD. NF was then manually filtered using a 1 mm mesh cloth, while EMD samples were filtered using the FD with 1 mm pore size. All samples were digested with collagenase prior to cell analysis. (A) Nucleated cell counts decreased by over half for NF and EMD processed samples, and further decreased with filtering, most notably for NF. (B) Nucleated cell viability remained >90% for all conditions. (C) The FD better maintained enrichment of cell types from EMD treatment, with overall higher percentages compared to MF (value=1) and NF filtered conditions. (D) Cell numbers were even greater for EMD/FD relative to filtered NF, particularly for total MSCs and the two subpopulations. Error bars represent standard error from at least three independent experiments. * indicates $p < 0.05$ relative to MF, ** indicates $p < 0.01$ relative to MF, and # indicates $p < 0.05$ relative to NF/filter based on both parametric and non-parametric tests.

Table 1:

Flow cytometry probe panel

Assay	Probe
CD34	Anti-CD34 Ab (clone 561)-BV421
CD45	Anti-CD45 Ab (clone 2D1)-BV510
SSEA-3	Anti-SSEA-3 Ab (clone MC-631)-FITC
CD26	Anti-CD26 Ab (clone BA5b)-PE
CD31	Anti-CD31 Ab (clone WM59)-PE/Cy7
CD55	Anti-CD55 Ab (clone JS11)-APC
CD13	Anti-CD13 Ab (clone WM15)-APC/Cy7
Viability	7-AAD

Table 2:

Stem and progenitor cell types of interest.

Cell type	Markers	Significance	References
CD34+	CD34+	Common marker for multipotentiality	38,46
Mesenchymal Stem Cells (MSCs)	CD45−, CD31−, CD34+	Key in regenerative wound healing	47
Endothelial Progenitor Cells (EPCs)	CD45−, CD31+, CD34+	Vascularization of healing tissues	48
Multilineage Differentiating Stress-Enduring (Muse)	CD45−, CD31−, CD34+, SSEA-3+, CD13+	Nontumorigenic, pluripotent, stress tolerant stem cells	23,25
DPP4+/CD55+	CD45−, CD31−, CD34+, CD26+, CD55+	Improved wound healing in diabetic models	24,49

Table 3:

Statistical analysis of EMD and FD processing results shown in Figure 5.

Outcomes	Mean (S.D.)			Parametric F test p-value	Post-hoc T tests			Non-parametric Kruskal Wallis test p-value
	MF	NF	EMD		EMD vs. MF	EMD vs. NF	NF vs. MF	
COUNT	898525 (329107)	130613 (103428)	271450 (58106)	0.0010	0.0045	0.6032	0.0012	0.0125
VIABILITY	90.8 (5.2)	90.5 (6.3)	92.6 (4.2)	0.8330	0.8823	0.8406	0.9959	0.7939
Population (%, normalized to MF)								
CD34		1.2 (0.3)	2.7 (1.3)	0.0745		0.0745		0.0209
MSC		1.3 (0.1)	1.9 (0.5)	0.0373		0.0373		0.0209
EPC		2.2 (0.2)	5.5 (3.1)	0.0755		0.0755		0.0209
MUSE		1.2 (0.6)	1.6 (0.3)	0.2580		0.2580		0.3865
DPP4		0.8 (0.4)	1.5 (0.4)	0.0393		0.0393		0.0209
Cell number (normalized to MF)								
CD34		0.2 (0.2)	0.9 (0.6)	0.0552		0.0552		0.0209
MSC		0.2 (0.1)	0.6 (0.2)	0.0197		0.0197		0.0209
EPC		0.3 (0.2)	1.8 (1.3)	0.0676		0.0676		0.0209
MUSE		0.2 (0.2)	0.5 (0.1)	0.0488		0.0488		0.0833
DPP4		0.1 (0.1)	0.5 (0.2)	0.0139		0.0139		0.0209